

Synthesis, in vitro and in silico Anti-Proliferative Studies of Novel Piperine-Oxadiazole and Thiadiazole Analogs

K. R. Amperayani^{a,*} and U. D. Parimi^a

^a Department of Chemistry, GVP Degree and PG College, Visakhapatnam, Andhra Pradesh, 530045 India

*e-mail: a.karteek.akrao@gmail.com

Received May 31, 2019; revised November 4, 2019; accepted November 5, 2019

Abstract—Piperine is a component of pepper which has earlier been reported as anticancer active compound. This work is emphasized on the design and synthesis of new hybrid piperine analogs by coupling piperine with the amine group of oxadiazoles and thiadiazoles. The new series of twelve piperine analogs was tested for in vitro anti-proliferative activity using sulforhodamine B (SRB) assay test against MCF-7, PC-3, and HeLa cell lines. Among the twelve synthesised molecules piperine derivative with oxadiazole bearing hydroxyl group (**3**) exhibits the higher activity against MCF-7 cell line than the reference drug Adriamycin and also displays the highest binding energy in the in silico studies. The other analogs are moderately active.

Keywords: piperine; oxadiazole; thiadiazoles; anti proliferative activity

DOI: 10.1134/S1070363219110227

INTRODUCTION

Application of natural products as anticancer agents is significantly developing due to their low side effects. Combination of natural products with synthetic drugs can produce hybrid molecules [1, 2] with low side effects and high biological activity. Such approach had been employed by us in the earlier studies [3] and led to positive results. So, we designed hybrid molecules of piperine with oxadiazole and thiadiazole as promising anticancer agents.

Some earlier studies on piperine proved its substantial anticancer effect [4] including prostate cancer [5], MCF-7 and A-549 [6], HeLa and breast cancer [7] and some more [8, 9]. The activity of piperine resides on the amide bond with the piperidine moiety [10]. Alterations in the amide bond can affect the biological activity of the entire molecule. Piperine derivatives could possess activity superior than the parent molecule [11, 12]. Piperine–amino acid ester conjugates showed good cytotoxic activity against human cancer cell lines [13]. Accordingly, we have modified the amide functionality of piperine for the following anti proliferative activity studies.

1,3,4-Oxadiazoles [14–16] and some thiadiazole [17–19] derivatives are promising molecules with diverse biological activities including anticancer. Based on the above, we have coupled the amine functional group of oxa

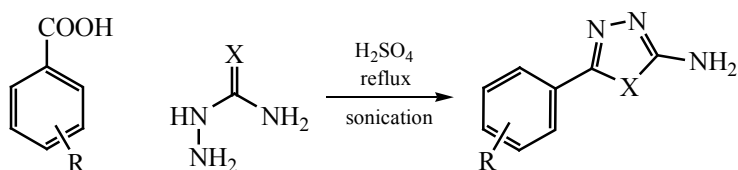
and thiadiazoles with piperic acid by the amide linkage for testing anti proliferative effect on MCF-7, PC-3, and HeLa cell lines. Actually, this is the first report on anti proliferative activity of piperine derivatives of oxadiazoles and thiadiazoles.

EXPERIMENTAL

All reagents were of AR grade and used directly without further purification. Piperine (97%) was purchased from Sigma Aldrich chemicals. Melting points were determined in open capillary tubes. FTIR spectra were recorded on a Perkin Elmer FTIR spectrophotometer using KBr pellets. ¹H and ¹³C NMR spectra were measured on a Bruker Avance 400 and 100 spectrometers respectively using TMS as an internal standard and CDCl₃ (¹H NMR) and CD₃OD (¹³C NMR) as solvents. HRMS were measured on a Bruker Micro TOF-Q II ESI spectrometer. Ultra sonication reactions were carried out on a PCI Analytics sonicator, frequency 25 KHz and power 220 W at room temperature. Progress of the reactions was monitored by TLC on Merck TLC silica gel plates using hexane: ethylacetate (3 : 2) mixture as an eluent. The spots were visualized under UV light.

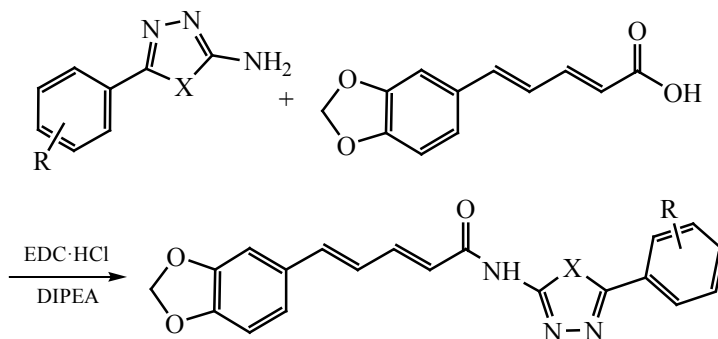
Piperic acid. Piperine (10 g) was dissolved in 300 mL of anhydrous ethanol containing 20% KOH and the mixture was refluxed upon stirring for 10 h to give the precipitate of potassium piperate, which was filtered

Scheme 1.



X = O or S; R = H, *p*-Cl, *p*-OH, *p*-NO₂, *o*-OH, *o*-NO₂.

Scheme 2.



PIP 1–12

X = O and S; R = H, *p*-Cl, *p*-NO₂, *o*-OH, *o*-NO₂.

off and washed with anhydrous ethanol. The precipitate was dissolved in distilled water and precipitated upon addition of HCl solution (0.1 M). The yellow precipitate of piperic acid was filtrated off and washed with distilled water (200 mL) to give powdery yellow piperic acid [20], yield 86.6%, mp 214–216°C.

Substituted oxadiazoles and thiadiazoles. A mixture of substituted benzoic acid (2 g) and 2 g of semicarbazide or thiosemicarbazide was dissolved in 10 mL of H₂SO₄ and subjected to ultrasonication for 30–45 min at room temperature (TLC). The product obtained was cooled down and poured onto crushed ice. The residue thus obtained was separated, washed with water, recrystallized from ethanol and chromatographed with hexane : ethylacetate to get the corresponding pure product (Scheme 1).

Coupling of piperine with oxadiazoles or thiadiazoles. The solution of 2.18 g of piperic acid in 20 mL of anhydrous CH₂Cl₂ was mixed with 1.92 g of 1-ethyl-3-(3-dimethylaminopropyl) carbodiimide HCl (EDC·HCl) and 2.60 mL of *N,N*-diisopropylethylamine (DIPEA) and stirred at 0–5°C. for 30 min. 1 mol of oxadiazole or thiadiazole derivative was added to the above mixture and stirred at room temperature for 2 h (TLC). After completion of the process (TLC), the reaction mixture was

washed with water (2×10 mL), aqueous solution of 1% H₃PO₄ (2×10 mL), an aqueous solution of 2.5% K₂CO₃ (2×10 mL), and concentrated to give the corresponding crude product. This was purified by column chromatography using hexane:ethylacetate as an eluent (Scheme 2).

(2*E*,4*E*)-5-(Benzo[*d*][1,3]dioxo-5-yl)-*N*-(5-phenyl-1,3,4-oxadiazol-2-yl)penta-2,4-dienamide (1). Brown crystals, yield 68%, mp 265°C. IR spectrum, ν , cm⁻¹: 1710 (amide CONH), 3100–3500 (amide NH). ¹H NMR spectrum, δ , ppm: 5.19 d.d (J = 14.7, 0.8 Hz, 1H), 6.01 d (J = 2.3 Hz, 1H), 6.07 d (J = 2.3 Hz, 1H), 6.66 d.d.d (J = 14.0, 7.0, 0.9 Hz, 1H), 6.70–6.82 m (2H), 6.82 d.d (J = 8.5, 1.9 Hz, 1H), 7.04 d (J = 1.8 Hz, 1H), 7.37–7.47 m (2H), 7.60–7.50 m (2H), 7.97–7.89 m (2H), 8.21 s (1H). ¹³C NMR spectrum, δ , ppm: 100.99, 106.96, 108.54, 120.68, 123.68, 126.01, 126.65, 126.74, 128.84, 130.40, 131.15, 138.30, 140.31, 147.05, 147.90, 152.42, 158.79, 168.74. HRMS: m/z : 362.1169 [H]⁺.

(2*E*,4*E*)-5-(Benzo[*d*][1,3]dioxol-5-yl)-*N*-[5-(4-chlorophenyl)-1,3,4-oxadiazol-2-yl]penta-2,4-dienamide (2). Brown crystals, yield 72%, mp 256°C. IR spectrum, ν , cm⁻¹: 1675 (amide CONH), 3100–3300 (amide NH). ¹H NMR spectrum, δ , ppm: 5.19 d.d (J = 14.7, 0.8 Hz, 1H), 6.01 d (J = 2.3 Hz, 1H), 6.07 d (J =

2.3 Hz, 1H), 6.66 d.d.d ($J = 14.0, 7.0, 0.9$ Hz, 1H), 6.82–6.70 m (2H), 6.82 d.d ($J = 8.5, 1.9$ Hz, 1H), 7.04 d ($J = 1.8$ Hz, 1H), 7.45 d.d ($J = 14.7, 7.1$ Hz, 1H), 7.47–7.55 m (2H), 8.03–8.11 m (2H), 8.21 s (1H). ^{13}C NMR spectrum, δ , ppm: 100.99, 106.96, 108.54, 120.68, 123.68, 126.01, 127.90, 128.38, 129.29, 130.40, 138.30, 138.60, 140.31, 147.05, 147.90, 152.42, 158.79, 168.74. HRMS: m/z : 396.1047 of $[\text{H}]^+$.

(2E,4E)-5-(benzo[d][1,3]dioxol-5-yl)-N-[5-(4-hydroxyphenyl)-1,3,4-oxadiazol-2-yl]penta-2,4-dienamide (3). Colourless crystals, yield 68%, mp 260°C. IR spectrum, ν , cm^{-1} : 1650 (CONH), 3100–3300 (amide NH). ^1H NMR spectrum, δ , ppm: 5.19 d.d ($J = 14.7, 0.9$ Hz, 1H), 6.10–6.02 m (2H), 6.66 d.d.d ($J = 14.0, 7.0, 0.8$ Hz, 1H), 6.70–6.79 m (1H), 6.79–6.86 m (2H), 7.07–6.94 m (3H), 7.34–7.27 m (1H), 7.35–7.51 m (2H), 8.16 s (1H), 9.10 s (1H). ^{13}C NMR spectrum, δ , ppm: 100.99, 106.96, 108.54, 111.69, 116.86, 119.02, 120.68, 123.68, 126.01, 128.97, 130.40, 133.70, 138.30, 140.31, 143.82, 147.05, 147.90, 158.75, 158.79, 168.74. HRMS: m/z : 378.2038 $[\text{H}]^+$.

(2E,4E)-5-(Benzo[d][1,3]dioxol-5-yl)-N-[5-(4-nitrophenyl)-1,3,4-oxadiazol-2-yl]penta-2,4-dienamide (4). Colorless crystals, yield 58%, mp 274°C. IR spectrum: 1700 (amide CONH), 3100–3500 (amide NH). ^1H NMR spectrum, δ , ppm: 5.19 d.d ($J = 14.7, 0.8$ Hz, 1H), 6.01 d ($J = 2.3$ Hz, 1H), 6.07 d ($J = 2.3$ Hz, 1H), 6.66 d.d.d ($J = 14.0, 7.0, 0.9$ Hz, 1H), 6.70–6.82 m (2H), 6.82 d.d ($J = 8.5, 1.9$ Hz, 1H), 7.04 d ($J = 1.8$ Hz, 1H), 7.45 d.d ($J = 14.7, 7.1$ Hz, 1H), 8.23 d.d ($J = 7.4, 1.0$ Hz, 3H), 8.37–8.45 m (2H). ^{13}C NMR spectrum, δ , ppm: 100.99, 106.96, 108.54, 120.68, 123.68, 124.12, 126.01, 127.58, 130.40, 132.07, 138.30, 140.31, 147.05, 147.90, 149.36, 152.42, 158.79, 168.74. HRMS: m/z : 407.0208 $[\text{H}]^+$.

(2E,4E)-N-[5-(2-Hydroxyphenyl)-1,3,4-oxadiazol-2-yl]-5-(benzo[d][1,3]dioxol-5-yl)penta-2,4-dienamide (5). Green crystals, yield 65%, mp 260°C. IR spectrum, cm^{-1} : 1675 (amide CONH), 3100–3300 (amide NH). ^1H NMR spectrum, δ , ppm: 5.19 d.d ($J = 14.7, 0.8$ Hz, 1H), 6.01 d ($J = 2.3$ Hz, 1H), 6.07 d ($J = 2.3$ Hz, 1H), 6.66 d.d.d ($J = 14.0, 7.0, 0.9$ Hz, 1H), 6.70–6.82 m (2H), 6.82 d.d ($J = 8.5, 1.9$ Hz, 1H), 6.94–7.07 m (3H), 7.27–7.34 m (1H), 7.40 t.d ($J = 7.6, 1.3$ Hz, 1H), 7.46 d.d ($J = 14.7, 7.1$ Hz, 1H), 8.16 s (1H), 9.10 s (1H). ^{13}C NMR spectrum, δ , ppm: 100.99, 106.96, 108.54, 111.69, 116.86, 119.02, 120.68, 123.68, 126.01, 128.97, 130.40, 133.70, 138.30, 140.31, 143.82, 147.05, 147.90, 158.75, 158.79, 168.74. HRMS: m/z : 378.0818 $[\text{H}]^+$.

(2E,4E)-5-(Benzo[d][1,3]dioxol-5-yl)-N-[5-(2-nitrophenyl)-1,3,4-oxadiazol-2-yl]penta-2,4-dienamide (6). Colourless crystals, yield 65%, mp 230°C. IR spectrum, ν , cm^{-1} : 1680 (amide CONH), 3200–3500 (amide NH). ^1H NMR spectrum, δ , ppm: 5.19 d.d ($J = 14.7, 0.8$ Hz, 1H), 6.01 d ($J = 2.3$ Hz, 1H), 6.07 d ($J = 2.3$ Hz, 1H), 6.66 d.d.d ($J = 14.0, 7.0, 0.9$ Hz, 1H), 6.70–6.82 m (2H), 6.82 d.d ($J = 8.5, 1.9$ Hz, 1H), 7.04 d ($J = 1.8$ Hz, 1H), 7.36–7.48 m (2H), 7.73 t.d ($J = 7.6, 1.3$ Hz, 1H), 7.79 d.d.d ($J = 12.6, 7.9, 1.3$ Hz, 2H), 8.14 s (1H). ^{13}C NMR spectrum, δ , ppm: 100.99, 106.96, 108.54, 120.68, 123.68, 125.71, 126.01, 126.59, 127.54, 128.77, 129.28, 130.40, 138.30, 140.31, 145.17, 146.16, 147.05, 147.90, 158.79, 168.74. HRMS: m/z : 407.0208 $[\text{H}]^+$.

(2E,4E)-5-(Benzo[d][1,3]dioxol-5-yl)-N-(5-phenyl-1,3,4-thiadiazol-2-yl)penta-2,4-dienamide. Grey crystals, yield 60%, mp 230°C. IR spectrum, cm^{-1} : 1690 (amide-CONH), 3100–3400 (amide NH). ^1H NMR spectrum, δ , ppm: 5.19 d.d ($J = 14.7, 0.8$ Hz, 1H), 6.01 d ($J = 2.3$ Hz, 1H), 6.07 d ($J = 2.3$ Hz, 1H), 6.66 d.d.d ($J = 14.0, 7.0, 0.9$ Hz, 1H), 6.70–6.82 m (2H), 6.82 d.d ($J = 8.5, 1.9$ Hz, 1H), 7.04 d ($J = 1.8$ Hz, 1H), 7.38–7.49 m (1H), 7.45–7.56 m (3H), 8.00–8.11 m (2H), 8.29 s (1H). ^{13}C NMR spectrum, δ , ppm: 100.99, 106.96, 108.54, 120.68, 123.68, 126.01, 127.34, 127.88, 130.27, 130.40, 133.75, 138.30, 140.31, 147.05, 147.90, 158.01, 163.17, 168.02. MS: (m/z): 378.2038 $[\text{H}]^+$.

(2E,4E)-5-(Benzo[d][1,3]dioxol-5-yl)-N-[5-(4-chlorophenyl)-1,3,4-thiadiazol-2-yl]penta-2,4-dienamide (8). Colourless crystals, yield 64%, mp 256°C. IR spectrum, ν , cm^{-1} : 1670 (amide CONH), 3100–3500 (amide NH). ^1H NMR spectrum, δ , ppm: 5.19 d.d ($J = 14.7, 0.8$ Hz, 1H), 6.01 d ($J = 2.3$ Hz, 1H), 6.07 d ($J = 2.3$ Hz, 1H), 6.66 d.d.d ($J = 14.0, 7.0, 0.9$ Hz, 1H), 6.70–6.79 m (1H), 6.79–6.86 m (2H), 7.04 d ($J = 1.8$ Hz, 1H), 7.40–7.52 m (3H), 7.87–7.95 m (2H), 8.22 s (1H). MS: m/z : 412.1078 $[\text{H}]^+$.

(2E,4E)-5-(Benzo[d][1,3]dioxol-5-yl)-N-[5-(4-hydroxyphenyl)-1,3,4-thiadiazol-2-yl]penta-2,4-dienamide (9). Colorless crystals, yield 58%, mp 280°C. IR spectrum, ν , cm^{-1} : 1690 (amide CONH), 3100–3500 (amide NH). ^1H NMR spectrum: δ , ppm: 5.19 d.d ($J = 14.7, 0.8$ Hz, 1H), 5.42 s (1H), 6.01 d ($J = 2.3$ Hz, 1H), 6.07 d ($J = 2.3$ Hz, 1H), 6.66 d.d.d ($J = 14.0, 7.0, 0.9$ Hz, 1H), 6.70–6.82 m (2H), 6.82 d.d ($J = 8.5, 1.9$ Hz, 1H), 6.87–6.95 m (2H), 7.04 d ($J = 1.8$ Hz, 1H), 7.45 d.d ($J = 14.7, 7.1$ Hz, 1H), 7.71–7.63 m (2H), 8.27 s (1H). ^{13}C NMR spectrum, δ , ppm: 100.99, 106.96, 108.54, 116.03,

120.68, 123.68, 125.00, 126.01, 128.78, 130.40, 138.30, 140.31, 147.05, 147.90, 158.01, 160.07, 163.17, 168.02. MS: m/z : 394.0970 [H]⁺⁺.

(2E,4E)-5-(Benzo[d][1,3]dioxol-5-yl)-N-[5-(4-nitrophenyl)-1,3,4-thiadiazol-2-yl]penta-2,4-dienamide (10). Brown crystals, yield 62%, mp 272°C. IR spectrum, ν , cm⁻¹: 1680 (amide CONH), 3100–3300 (amide NH). ¹H NMR spectrum, δ , ppm: 5.19 d.d (J = 14.7, 0.8 Hz, 1H), 6.01 d (J = 2.3 Hz, 1H), 6.07 d (J = 2.3 Hz, 1H), 6.66 d.d.d (J = 14.0, 7.0, 0.9 Hz, 1H), 6.70–6.82 m (2H), 6.82 d.d (J = 8.5, 1.9 Hz, 1H), 7.04 d (J = 1.8 Hz, 1H), 7.45 d.d (J = 14.6, 7.0 Hz, 1H), 8.16–8.24 m (2H), 8.29–8.40 m (3H). ¹³C NMR spectrum, δ , ppm: 100.99, 106.96, 108.54, 120.68, 123.68, 123.86, 126.01, 127.21, 130.40, 138.30, 139.45, 140.31, 147.05, 147.90, 149.37, 158.01, 163.17, 168.02. MS: m/z : 423.1164 [H]⁺.

(2E,4E)-5-(Benzo[d][1,3]dioxol-5-yl)-N-[5-(2-hydroxyphenyl)-1,3,4-thiadiazol-2-yl]penta-2,4-dienamide (11). Grey crystals, yield 64%, mp 286°C. IR spectrum, ν , cm⁻¹: 1690 (amide-CONH), 3100–3400 (amide NH). ¹H NMR spectrum, δ , ppm: 5.19 d.d (J = 14.7, 0.8 Hz, 1H), 6.01 d (J = 2.3 Hz, 1H), 6.07 d (J = 2.3 Hz, 1H), 6.66 d.d.d (J = 14.0, 7.0, 0.9 Hz, 1H), 6.70–6.82 m (2H), 6.82 d.d (J = 8.5, 1.9 Hz, 1H), 6.88–7.03 m (2H), 7.04 d (J = 1.8 Hz, 1H), 7.30 d.d (J = 7.8, 1.2 Hz, 1H), 7.40 t.d (J = 7.7, 1.3 Hz, 1H), 7.46 d.d (J = 14.7, 7.1 Hz, 1H), 7.78 s (1H), 8.23 s (1H). ¹³C NMR spectrum, δ , ppm: 100.99, 108.54, 116.66, 119.44, 120.68, 123.16, 123.68, 126.01, 127.61, 129.20, 130.40, 138.30, 140.31, 147.05, 147.90, 156.27, 157.41, 158.01, 168.02. MS: m/z : 394.1161 [H]⁺.

(2E,4E)-5-(Benzo[d][1,3]dioxol-5-yl)-N-[5-(2-nitrophenyl)-1,3,4-thiadiazol-2-yl]penta-2,4-dienamide (12). Colorless crystals, yield 64%, mp 284°C. IR spectrum, ν , cm⁻¹: 1665 (amide CONH), 3100–3400 (amide NH). ¹H NMR spectrum, δ , ppm: 5.19 d.d (J = 14.7, 0.8 Hz, 1H), 6.01 d (J = 2.3 Hz, 1H), 6.07 d (J = 2.3 Hz, 1H), 6.66 d.d.d (J = 14.0, 7.0, 0.9 Hz, 1H), 6.70–6.82 m (2H), 6.82 d.d (J = 8.5, 1.9 Hz, 1H), 7.04 d (J = 1.8 Hz, 1H), 7.27 d.d.d (J = 7.9, 7.3, 1.3 Hz, 1H), 7.35–7.48 m (3H), 7.74 d.d (J = 7.9, 1.4 Hz, 1H), 8.26 s (1H). ¹³C NMR spectrum, δ , ppm: 100.99, 106.96, 108.54, 120.68, 123.68, 126.01, 126.03, 127.59, 130.40, 130.82, 131.86, 132.39, 133.84, 138.30, 140.31, 147.05, 147.90, 158.01, 163.42, 168.02. MS: m/z : [H]⁺.

SRB assay. The cell lines were grown in RPMI 1640 medium containing 10% fetal bovine serum and 2 mM L-glutamine. Cells were inoculated into 96 well microtiter

plates in 100 μ L at plating densities, depending on the doubling time of individual cell line. After cell inoculation, the microtiter plates were incubated at 37°C, 5% CO₂, 95% air and 100% relative humidity for 24 h prior to addition of experimental drugs [21, 22]. Experimental drugs were initially solubilized in DMSO at 100 mg/mL and diluted to 1 mg/mL using water and stored frozen prior to use. At the time of drug addition, an aliquot of frozen concentrate (1 mg/mL) was diluted to 100, 200, 400, and 800 μ g/mL with complete medium containing test article. Aliquots of 10 μ L of these different drug dilutions were added to the appropriate microtiter wells already containing 90 μ L of medium, resulting in the required final drug concentrations 10, 20, 40, and 80 μ g/mL. After addition of the compound, plates were incubated at standard conditions for 48 h and assay was terminated by the addition of cold TCA. Cells were fixed in situ by the gentle addition of 50 μ L of cold 30% (w/v) TCA (final concentration, 10% TCA) and incubated for 60 min at 4°C. The supernatant was discarded; the plates were washed five times with tap water and air dried. Sulforhodamine B (SRB) solution (50 μ L) at 0.4% (w/v) in 1% acetic acid was added to each of the wells, and plates were incubated for 20 min at room temperature. After staining, unbound dye was recovered and the residual dye was removed by washing five times with 1% acetic acid. The plates were air dried. Bound stain was subsequently eluted with 10 mM trizma base, and the absorbance was read on a plate reader at a wavelength of 540 nm with 690 nm reference wavelength.

Percent growth was calculated on a plate-by-plate basis for test wells relative to control wells. Percent growth was expressed as the ratio of average absorbance of the test well to the average absorbance of the control wells \times 100. Using the six absorbance measurements [time zero (Tz), control growth (C), and test growth in the presence of drug at the four concentration levels (Ti)]; the percentage growth was calculated at each of the drug concentration levels. Percentage growth inhibition was calculated as: $[(Ti/C) \times 100\%]$.

In silico docking. The possible docking modes between the piperine analog and cancer cell lines 3EU7 [23] for MCF-7 (Human breast cancer protein), 1Z8I [24] for PC-3 cell line (Human prostate cancer) and 1XQH [25] for HeLa cell line (Cervical cancer) was studied using Autodock 2.0 software. The lead molecules were designed using ChemDraw software and used to analyze the binding affinity with the cancer proteins. Crystal structure of all the cancer cell lines was downloaded from

Protein Data Bank website (<http://www.rcsb.org>) as PDB format and converted to PDBQT format. We have taken Lamarckian genetic algorithm (LGA) for ligand conformations. An extended PDB format, termed as PDBQT file was used for coordinate ligand and macromolecule which includes atomic partial charges, polar bonds and hydrogen bonds. An AutoDock tool was used for creating PDBQT files from traditional PDB files. AutoDock was run several times to get various docked conformations, and used to analyze the predicted docking energy. AutoDock tools provide various parameters to analyze the results of docking simulations such as binding energy, ligand efficiency, inhibition constant and intramolecular energy. For each ligand, ten best conformations were generated and scored using AutoDock 4.2 scoring functions.

RESULTS AND DISCUSSION

All the novel molecules were characterized by FT-IR, ^1H and ^{13}C NMR, and Mass spectral data. Formation of new compounds was confirmed by the amide bond ^1H NMR characteristic singlet in the range of 9.15–9.75 ppm, IR broad amide N–H stretching frequency band at 3300–3500 cm^{-1} and amide C=O stretching frequency band in the range of 1630–1680 cm^{-1} .

In vitro anti-proliferative activity. Anti-proliferative activity of newly synthesised piperine analogs **1–12** was screened against three cell lines MCF-7, PC-3, and HeLa using sulforhodamine B (SRB) colorimetric assay (Table 1). The growth inhibitory concentration (GI_{50}) values were compared with the standard drugs Adriamycin. All tested molecules demonstrated high to moderate anti-proliferative activity. Among the entire series of molecules piperine oxadiazole analog **3** exhibited very high activity against MCF-7. The compounds **5** and **9** were also characterized by a noteworthy activity against MCF-7 cancer cell lines. Remaining compounds showed moderate activity against MCF-7, PC-3, and HeLa cell lines. Some compounds **4**, **10**, and **12** were found to be inactive against all cell lines. The anti proliferative activity of piperine analog **3** might be due to the presence of the electron donating hydroxyl group on the benzene ring which was characterized by strong hydrogen bonding with protein molecule. Inactivity of some compounds could be due to the presence of electron withdrawing groups that could not form hydrogen bonds with the protein. The accumulated data indicated that inhibition of cells growth was concentration dependent. Docking studies

Table 1. In vitro anti-proliferative activity of piperine derivatives

Compound	GI_{50}^a , $\mu\text{g/mL}$		
	MCF-7	PC-3	HeLa
1	28.2	50.9	50.1
2	>80	64.3	66.8
3	2.0	48.0	48.0
4	>80	>80	>80
5	18.6	>80	>80
6	27.4	78.1	62.3
7	23.2	>80	>80
8	36.7	58.8	60.1
9	12.9	38.5	33.4
10	>80	>80	>80
11	39.8	41.8	43.4
12	>80	>80	>80
Piperine	11.75	12.8	14.5
Adriamycin	<10	<10	<10

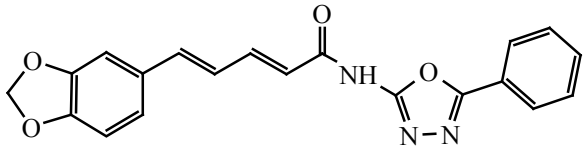
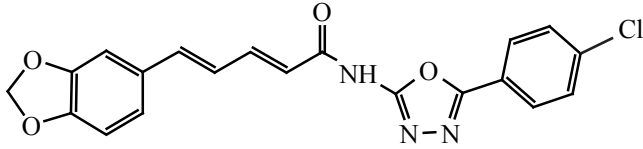
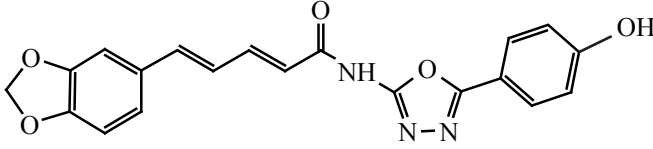
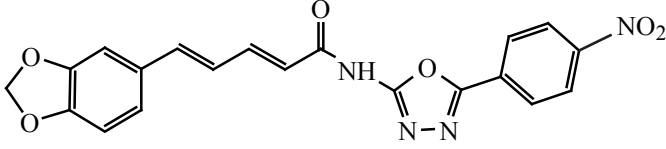
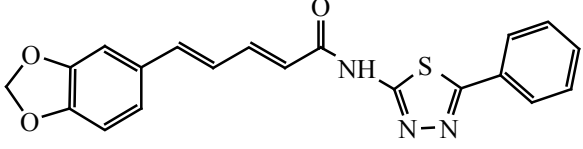
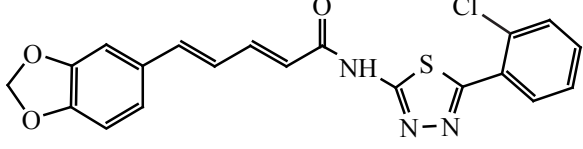
^a (GI_{50}) is a concentration of drug causing 50% inhibition of cell growth.

also singled out the derivative **3** as the most active with the highest binding energy -15.23 kcal/mol.

In silico molecular docking. The synthesized piperine analogs **1–12** were used as the objects of molecular docking studies. The targeted molecules were docked against the cancer cell lines 3EU7 for MCF-7 (Human Breast cancer protein), 1Z8I for PC-3 cell line (Human prostate cancer) and 1XQH for HeLa cell line (Cervical cancer) using Autodock 4.2 software (Table 2).

According to the in silico studies it was determined that compound **3** could adopt a “U-shape” conformation in the pocket of the 3EU7 protein molecule, and the 4-hydroxyphenyl group was surrounded by the residues of Val-200, Try-300, Ala-278, and Phe-300, forming a structure stabilized by H-bonding. The estimated binding energy of the target molecule also showed strong binding towards the protein moiety probably due to the presence of the rigid molecule with amide linkage and hydroxyl groups on heterocyclic moiety.

Table 2. Binding energies between the representative piperine derivatives **1–4**, **7**, **12**, and MCF-7, PC3, and HeLa

Compound no.	Structure of compounds	Binding energy, kcal/mol		
		MCF-7	PC-3	HeLa
1		-13.54	-9.56	-12.92
2		-13.87	-9.83	-12.92
3		-15.23	-10.83	-13.22
4		-13.63	-9.13	-13.14
7		-14.06	-9.08	-13.25
12		-13.88	-5.83	-13.68

CONCLUSIONS

A novel series of piperine analogs with oxadiazoles and thiadiazoles is synthesized by coupling the natural product piperine with amine substituted oxadiazoles and thiadiazoles. The products have been tested for their anti proliferative activity against three cell lines MCF-7, PC-3, and HeLa. Among the entire synthesized analogs piperine derivative **3** with oxadiazole bearing the hydroxyl group has been determined to be a potent anticancer agent against MCF-7 cell line with binding energy of -15.23 kcal/mol. All the remaining compounds are moderately active against the tested cell lines. The results are in accord with the in silico studies.

ACKNOWLEDGMENTS

We also thank for in vitro SRB assay for the anti-cancer activity, at Anti-Cancer Drug screening facility (ACDSF), ACTREC, Tata Memorial Centre, Navi Mumbai on hiring basis.

REFERENCES

- Melanie, L. and Luisa, H., *Int. J. Med. Chem.*, 2015, vol. 25, p. 23.
<https://doi.org/10.1155/2015/458319>
- Marie-H., Teiten, M.D., and Marc, D., *Molecules*. 2014, vol. 19, p. 20839.
<https://doi.org/10.3390/molecules191220839>
- Durvasula Venugopal, V.R., Nagendra Sastry, Y., and Umadevi, P., *Anticancer Agents Med. Chem.*, 2014, vol. 4, p. 606.
<https://doi.org/10.4172/2161-0444.1000201>

4. Bezerra, D.P., Castro, F.O., Alves, A.P.N.N., Pessoa, C., Moraes, M.O., Silveira, E.R., Lima, M.A.S., Elmira, F.J.M., and Costa-Lotuf, L.V., *Brazilian J. Med. Biol. Res.*, 2006, vol. 39, p. 599.
<https://doi.org/10.1002/jat.1311>
5. Abhilash S., Aditya V.S., Gajalakshmi D., Mary M.B., Gary L.J., Brian W., Guoxing Z., Aoshuang C., Ramaswamy K., and Gnanasekar M., *Plos One*, 2013, vol. 8, no. 6, p. e65889.
<https://doi.org/10.1371/journal.pone.0065889>
6. Li, S., Lei, Y., Jia, Y., Li, N., Wink, M., and Ma, Y., *Phytomedicine*, 2011, vol. 19, p. 83.
<https://doi.org/10.1016/j.phymed.2011.06.031>
7. Padmaa, M., Paarakh, D.C., Sreeram Shruthi, S.D., Sujana, P.S., and Ganapathy., *J. Med. Pharm. Sci.* 2015, vol. 1, p. 9.
<https://doi.org/10.36348.SJMPS>
8. Do, M.T., Kim, H.G., Choi, J.H., Khanal, T., Park, B.H., Tran, T.P., Jeong, T.C., and Jeong, H.G., *Food Chem.*, 2013, vol. 141(3), p. 2591.
<https://doi.org/10.1016/j.foodchem.2013.04.125>
9. Makhov, P., Golovine, K., Canter, D., Kutikov, K., Simhan, J., Corlew, M.M., Uzzo, R.G., and Kolenko, V.M., *Prostate*. 2012, vol. 72(6), p. 661.
<https://doi.org/10.1002/pros.21469>
10. Singh, I.P., and Choudhary, A., *Current Top Med Chem.*, 2015, vol. 15 (17), p. 1722.
<https://doi.org/10.1002/pros.21469>
11. Umadevi, P., Deepti. K., and Venugopal, D.V.R., *Med. Chem. Res.*, 2013, vol. 22, p. 5466.
<https://doi.org/10.1007/s00044-013-0541-4>
12. Venkatasamy. R., Faas. L., Young, A.R., Ramana. A., and Hidera, R.C., *Bioorg. Med. Chem.*, 2004, vol. 12, p. 1905.
<https://doi.org/10.1016/j.bmc.2004.01.036>
13. Subba Rao, V.R., Suresh, G., Ranga Rao, R., Suresh Babu, K., Chashoo, G., Saxena, A.K., and Madhusudana Rao, *J. Med Chem Res.*, 2012, vol. 21, p. 38.
<https://doi.org/10.1007/s00044-010-9500-5>
14. Mamdouh, A.Z., Abu-Zaied, Galal, A.M.N., Randa, H.S., Shahinaz, H., and Sayed, *Pharmacol. Pharm.*, 2012, vol. 3, p. 254.
<https://doi.org/10.4236/pp.2012.32034>
15. Kumar, D., Sundaree, S., Johnson, E.O., and Shah, K., *Bioorg. Med. Chem. Lett.*, 2009, vol. 19(15), p. 4492.
<https://doi.org/10.1016/j.bmcl.2009.03.172>
16. Rakesh, R.S., Shubhada, C., Shamal, P., Vetale., Dinesh, T., Makhija., Prabhaka, Y., and Shirodkar, R., *Int. J. Pharm. Tech. Res.*, 2013, vol. 5, p. 1233.
17. Asif H., Rashid, MD., Mishra, R., Shama, P., and Dong-SooShin., *Bioorg. Med. Chem. Lett.*, 2012, vol. 22(17), p. 5438.
<https://doi.org/10.1016/j.bmcl.2012.07.038>
18. Yang, X.H., Wen, Q., Zhao, T.T., Sun, J., Li, X., Xing, M., Lu, X., and Zhu, H.L., *Bioorg. Med. Chem.*, 2012, vol. 20(3), p. 1181.
<https://doi.org/10.1016/j.bmc.2011.12.057>
19. Matysiak, J., and Opolski, A., *Bioorg. Med. Chem.*, 2006, vol. 14, p. 4483.
<https://doi.org/10.1016/j.bmc.2006.02.027>
20. Vanicha V., and Kirtikara, K., *Nature Protocols*, 2006, vol. 1, p. 1112.
<https://doi.org/10.1038/nprot.2006.179>
21. Skehn, P., Storeng, R., Scudiero. A., Monks. J., McMahon. D., Vistica. D., Jonathan. T.W., Bokesch, H., Kenney, S., and Boyd, M.R., *J. Nat. Cancer. Inst.* 1990, vol. 82, p. 1107.
<https://doi.org/10.1093/jnci/82.13.1107>
22. Oliver, A.W., Swift, S., Lord, C.J., Ashwort, A., and Pearl, L.H., *Embo Rep.* 2009, vol. 10, p. 990.
<https://doi.org/10.1038/embor.2009.126>
23. Bobofchak, K.M., Pineda, A.O., Mathews, F.S., and Di Cera, E., *J. Biol. Chem.* 2005, vol. 280, p. 25644.
<https://doi.org/10.1074/jbc.M503499200>
24. Chuikov, S., Kurash, J.K., Wilson, J.R., Xiao, B., Justin, N., Ivanov, G.S, McKinney, K., Tempst, P., Prives, C., Gambelin, S.J., Barlev, N.A., and Reinberg, D., *Nature*, 2004, vol. 432, p. 353.
<https://doi.org/10.1038/nature03117>
25. Khodade, P., Prabhu, R., and Chandra, N., *J. App. Crystal*, 2007, vol. 40, p. 598.
<https://doi.org/10.1107/S0021889807011053>